Unified analytical description of the time evolution of decay for initial states formed by wave-packet scattering and by initial decaying states in quantum systems

Sergio Cordero,[1,*] Gastón García-Calderón,[2,†] Roberto Romo,[3,‡] and Jorge Villavicencio[3,§]

[1]*Instituto de Ciencias Físicas, Universidad Nacional Autónoma de México, Apartado postal 48-3, Cuernavaca, Morelos 62251, México*

[2]*Instituto de Física, Universidad Nacional Autónoma de México, Apartado Postal 20 364, 01000 México, D.F., México*

[3]*Facultad de Ciencias, Universidad Autónoma de Baja California, Apartado Postal 1880, 22800 Ensenada, Baja California, México*

(Received 1 September 2011; published 24 October 2011)

We consider a unified analytical approach for scattering and decay processes in one-dimensional resonant tunneling systems using the formalism of resonant states to address the issue of the differences and similarities in the time evolution of decay between the decay of an arbitrary state prepared initially within a system and the formation and subsequent decay of a quasistationary state in the scattering of a Gaussian wavepacket on that system. We find three distinctive regimes. A first regime, which refers only to the quasistationary state, that is characterized by a buildup time of the probability density at a given position within the internal region of the potential. Here we find that the buildup time has a dependence on position. A second regime, dominated by the exponentially decaying terms, where the decay of the quasistationary state proceeds in an almost identical fashion as for the initially prepared decaying state. And finally, a third regime that involves the transition to nonexponential decay at long times and its ulterior behavior as an inverse power of time. Here we find that the time scale of the transition occurs at different times, which implies a dependence on the parameters of the initial state.

DOI: 10.1103/PhysRevA.84.042118 PACS number(s): 03.65.−w, 73.21.Cd, 73.40.Gk

I. INTRODUCTION

The simple theoretical treatments of quantum decay usually refer to a particle confined initially by a barrier within an interaction region from which it escapes via tunneling. The early studies on α decay in radioactive nuclei, which led to the derivation of the exponential decay law, were in fact based on such simple models [1–3]. There, since the lifetime of these systems is extremely large, the mode of formation of the initial state is irrelevant [4]. It soon became clear that scattering processes may allow us to study the formation and the decay of unstable or quasistationary states. This has been usually studied in a time-independent framework and refers to systems where the lifetime is very short. In this case, the quasistationary state manifests itself as a sharp resonance in the cross section having a Lorentzian or Breit-Wigner shape, where the width of the resonance is inversely proportional to the lifetime of the state [4]. Subsequent work by Khalfin at the end of the 1950s and since then by a number of authors pointed out the approximate validity of the exponential decay law in systems whose energy spectra is bounded from below, i.e., $E \in (0,\infty)$ [5]. It was argued that, in general, deviations from the exponential decay law were expected at very short or very long times compared with the lifetime of the system. These theoretical predictions have been confirmed by experiment in recent years [6,7].

In present times, the possibility of designing artificial quantum structures [8] has opened new ways to study the time evolution of scattering and decay in quantum systems. One possible way to create the initial state in artificial one-dimensional semiconductor structures is, for example, by laser excitation [9–11], that it is usually assumed to be an instantaneous process, where the decaying particle seats in one of the quantum wells of the system. Another way of creating the initial state is via a scattering mechanism. There, decay is preceded by a buildup process of the electronic probability density inside the system [12,13].

Most of the theoretical treatments of decay do not incorporate into the description the formation of the initial state, a point of view compatible with the former of the two processes mentioned above. The scattering approach, on the other hand, describes on the same footing the formation and subsequent decay of the quasistationary state formed inside the system. The Gaussian wave packet scattered by a one-dimensional resonant tunneling system has been the model used to analyze in this fashion the dynamics of the formation and decay of a quasistationary state [12–15]. In particular, Støvneng and Hauge [13] studied the dynamics of resonant tunneling through a double barrier system using the tight-binding model. They focused their work in analyzing the buildup time of the probability density inside the system and found that it is directly related to the spatial width of the wavepacket and that, in general, it differs from the decay time. The work of Peisakhovich and Shtygashev [14,15] addresses the formation and decay of a quasistationary state on a finite lattice and exemplify their findings by solving a periodic system formed by N identical δ potentials. They consider an approximate numerical approach involving the steepest descent and residue theory methods. In this work we consider a resonant state formalism [16,17] to compare in a unified form the process of formation and subsequent decay of a quasistationary state by scattering of a Gaussian wavepacket in one-dimensional resonant systems and the decay of an arbitrary state prepared initially within such systems. Our aim is to elucidate the common features as well as the relevant differences in both cases.

*cordero@fis.unam.mx
†gaston@fisica.unam.mx
‡romo@uabc.edu.mx
§villavics@uabc.edu.mx

The paper is organized as follows. Section II provides a brief review of the resonant state formalism. It involves two subsections: Sec. II A discusses the time evolution of decay of an initial arbitrary state for a potential; Sec. II B refers to the scattering of a Gaussian wavepacket to describe the formation and decay of a quasistationary state along the internal region of a potential. Section III deals with two examples and its discussion: Sec. III A, the double barrier system; Sec. III B, the quadruple barrier system. Finally, Sec. IV presents the concluding remarks.

II. FORMALISM

In this section we establish the notation to be used along the paper and present the formalism employed to describe the time evolution of decay. Our problem deals with solving the time-dependent Schrödinger equation in one dimension,

$$\left[i\hbar\frac{\partial}{\partial t}-\mathcal{H}\right]\Psi(x,t)=0, \tag{1}$$

for a given arbitrary initial state $\Psi(x,0)$, where the Hamiltonian $\mathcal{H}$ of the system, for a particle of effective mass m, is defined as

$$\mathcal{H}=-\frac{\hbar^2}{2m}\frac{\partial^2}{\partial x^2}+\mathcal{V}(x), \tag{2}$$

corresponding to an arbitrary finite range one-dimensional potential $\mathcal{V}(x)$, i.e., $\mathcal{V}(x)=0$ for $x<0$ and $x>L$.

We obtain analytically solutions $\Psi(x,t)$ of Eq. (1) along the internal region ($0<x<L$), for different ways of preparing the initial state $\Psi(x,0)$. We consider two interesting cases: (i) the *purely decaying* case, where $\Psi(x,0)$ is seated inside the interaction region as a localized pulse in a quantum well, and (ii) the *scattering and decay* case, where $\Psi(x,0)$ is an incident cutoff Gaussian wave packet. Since $\Psi(x,0)$ comes from outside the interaction region in the latter case, the decay is preceded by a buildup process of the electronic probability density inside the system.

In the next subsections, we present a résumé of the analytical procedures leading to the formal solutions $\Psi(x,t)$ for each of the above-mentioned cases. Both approaches are based on a resonance formalism in one-dimension that invokes the analytical properties of the outgoing Green's function $G^+(x,x';k)$ of the problem. Resonance expansions of G^+ in terms of its complex poles $\kappa_n=\alpha_n-i\beta_n$ distributed along the third and fourth quadrants of the complex k plane in a well-known manner [18] are used to obtain formal expressions for the solutions.

A. Decay problem

For the purely decay problem, let us consider that, at the time $t=0$, the initial state of the particle, $\Psi(x,0)$, is arbitrary but confined within the internal region of the potential $\mathcal{V}(x)$. The solution at a later time $t>0$ may be expressed in terms of the retarded Green's function $g(x,x';t)$ as

$$\Psi_d(x,t)=\int_0^L g(x,x';t)\,\Psi_d(x',0)\,dx',\quad t>0. \tag{3}$$

In order to obtain an analytical expression for the wavefunction given by Eq. (3), we must first evaluate the retarded Green's function $g(x,x';t)$. One may proceed by relating $g(x,x';t)$ with its corresponding outgoing Green's function $G^+(x,x',k)$ using the Laplace transform method in momentum k space [19], which yields

$$g(x,x';t)=\left(\frac{\hbar^2}{2m}\right)\frac{i}{2\pi}\int_{-\infty}^{\infty}G^+(x,x';k)e^{-i\hbar k^2t/2m}\,2k\,dk. \tag{4}$$

Following the work by García-Calderón [20], we obtain an expansion of $G^+(x,x';k)$ involving its complex poles $\{\kappa_n\}$, and their corresponding residues, which are proportional to the resonance eigenfunctions $\{u_n(x)\}$ [21],

$$G^+(x,x';k)=\left(\frac{2m}{\hbar^2}\right)\frac{1}{2k}\sum_{n=-\infty}^{\infty}\frac{u_n(x)u_n(x')}{k-\kappa_n}. \tag{5}$$

The above expansion holds for $0\leqslant(x,x')^{\ddagger}\leqslant L$, where the symbol $\ddagger$ indicates the fact that the expansion is valid for all values x, x' in the interval $[0,L]$, except when $x=x'=0$ or $x=x'=L$. The resonance functions $u_n(x)$ satisfy the stationary Schrödinger's equation of the problem with complex eigenvalues, i.e.,

$$[E_n-\mathcal{H}]\,u_n(x)=0,\qquad E_n=\frac{\hbar^2\kappa_n^2}{2m}. \tag{6}$$

They obey outgoing boundary conditions at $x=0$ and $x=L$, given, respectively, by

$$\begin{aligned}\left.\frac{d}{dx}u_n(x)\right|_{x=0}&=-i\kappa_nu_n(0),\\ \left.\frac{d}{dx}u_n(x)\right|_{x=L}&=i\kappa_nu_n(L).\end{aligned} \tag{7}$$

Notice that the complex poles κ_{-n}, seated on the third quadrant of the complex k plane satisfy, from time-reversal considerations, $\kappa_{-n}=-\kappa_n^*$. Similarly, the corresponding resonant states $u_{-n}(x)$ satisfy $u_{-n}(x)=u_n^*(x)$. The complex energy poles may also be written as $E_n=\mathcal{E}_n-i\Gamma_n/2$ and, hence, $\mathcal{E}_n=\hbar^2(\alpha_n^2-\beta_n^2)/2m$ and $\Gamma_n=\hbar^2(4\alpha_n\beta_n)/2m$. The $u_n(x)$ are also proportional to the residues of the function $G^+(x,x';k)$ [21] around the complex poles κ_n [Eq. (5)],which provides the normalization condition for resonance states [17,19,21]:

$$\int_0^L u_n^2(x)\,dx+i\,\frac{u_n^2(0)+u_n^2(L)}{2\kappa_n}=1. \tag{8}$$

The resonance states $\{u_n(x)\}$ also fulfill the closure relationship,

$$\frac{1}{2}\sum_{n=-\infty}^{\infty}u_n(x)\,u_n(x')=\delta(x-x');\ \ 0\leqslant(x,x')^{\ddagger}\leqslant L, \tag{9}$$

and the sum rule,

$$\sum_{n=-\infty}^{\infty}\frac{u_n(x)\,u_n(x')}{\kappa_n}=0;\ \ 0\leqslant(x,x')^{\ddagger}\leqslant L. \tag{10}$$

The set of $\{\kappa_n\}$ and the corresponding $\{u_n(x)\}$ that follow from the solution of the above complex eigenvalue problem may be obtained by well-known methods [21].

Substituting Eq. (5) into Eq. (4), we obtain a resonance expansion of $g(x,x';t)$:

$$g(x,x';t) = \sum_{n=-\infty}^{\infty} u_n(x)u_n(x')\,M(y_n). \tag{11}$$

In the above infinite sum, the resonance functions u_n deal with the spatial features along the internal region, while the time evolution is given by the Moshinsky functions (or M functions) $M(y_q)$, defined as

$$M(y_q) = \frac{i}{2\pi}\int_{-\infty}^{\infty}\frac{e^{-i\hbar k^2 t/2m}}{k-\kappa_q}dk = \frac{1}{2}\omega(iy_q), \tag{12}$$

where

$$y_q = -\exp(-i\pi/4)\sqrt{\frac{\hbar}{2m}}\kappa_q t^{1/2}, \tag{13}$$

with $q = \pm 1, \pm 2, \ldots \pm n$ and $\omega(z) = \exp(-z^2)\mathrm{erfc}(-iz)$ stands for the well-known Faddeyeva function [22,23].

Feeding Eq. (11) into Eq. (3) and using Eq. (12), one arrives to an expression for the time-dependent wavefunction $\Psi_d(x,t)$ along the internal region $[0,L]$ of the potential, namely,

$$\Psi_d(x,t) = \frac{1}{2}\sum_{n=-\infty}^{\infty} C_n\,u_n(x)\,\omega(iy_n), \tag{14}$$

where the expansion coefficients are given by

$$C_n = \int_0^L \Psi(x,0)u_n(x)\,dx. \tag{15}$$

The C_n fulfill useful relationships similar to Eqs. (9) and (10):

$$\mathrm{Re}\left(\sum_{n=1}^{\infty} C_n\bar{C}_n\right) = 1, \tag{16}$$

and

$$\mathrm{Im}\left(\sum_{n=1}^{\infty}\frac{C_n\bar{C}_n}{k_n}\right) = 0, \tag{17}$$

where in the above expressions $\bar{C}_n$ is defined as

$$\bar{C}_n = \int_0^L \Psi^*(x,0)\,u_n(x)\,dx. \tag{18}$$

In the above expression, the relationship $C_{-n}\bar{C}_{-n} = (C_n\bar{C}_n)^*$ has been used. Notice that, if $\Psi_d(x,0)$ is real, then $\bar{C}_n = C_n$.

It is convenient to rewrite Eq. (14) using the symmetry relations $u_{-n} = u_n^*$ and $\kappa_{-n} = -\kappa_n^*$, as well as the symmetry relation for the Faddeyeva functions [22,23],

$$\omega(iz) = 2e^{-z^2} - \omega(-iz), \tag{19}$$

to obtain

$$\Psi_d(x,t) = \sum_{n=1}^{\infty} C_n u_n(x)e^{-i\mathcal{E}_n t/\hbar}e^{-\Gamma_n t/2\hbar} + R_n(x,t), \tag{20}$$

which exhibits explicitly the exponential decay behavior of the wavefunction. The term $R_n(x,t)$ in Eq. (20) stands for the nonexponential contribution, which becomes a relevant contribution both at very short and very long times compared with the lifetime of the system. It may be shown that at very long times $\Psi_d(x,t) \sim 1/t^{3/2}$ [16,17].

In particular, as discussed in Ref. [24], the expression for the wavefunction in the case of a multibarrier system with minibands having M-resonance levels each, i.e., a system with $M+1$ barriers, may be written as

$$\Psi_d(x,t) \approx \sum_{n=1}^{M} C_n u_n(x)e^{-i\mathcal{E}_n t/\hbar}e^{-\Gamma_n t/2\hbar}. \tag{21}$$

Hence, the corresponding probability density $|\Psi(x,t)|^2$ may be written as

$$|\Psi_d(x,t)|^2 \approx \rho_d^{\exp}(x,t) + I_d^{\mathrm{Rabi}}(x,t), \tag{22}$$

where $\rho_d^{\exp}(x,t)$ stands for purely exponentially decaying contributions,

$$\rho_d^{\exp}(x,t) = \sum_{n=1}^{M}|C_n|^2|u_n(x)|^2e^{-\Gamma_n t/\hbar}, \tag{23}$$

and $I_d^{\mathrm{Rabi}}(x,t)$ describes the interference contribution formed by decaying Rabi-type oscillatory contributions,

$$I_d^{\mathrm{Rabi}}(x,t) = 2\sum_{n,m>n}^{M}|C_m^*C_n u_m^*(x)u_n(x)|e^{-\bar{\Gamma}_{mn}t/\hbar} \times\cos[\Phi_{mn}(x,t)], \tag{24}$$

with

$$\Phi_{mn}(x,t) = \Omega_{mn}t + \theta_{mn}(x) + \vartheta_{mn}, \tag{25}$$

where the different phases above are defined through the expressions $u_m^*(x)u_n(x) = |u_m^*(x)u_n(x)|\exp[i\theta_{mn}(x)]$, $C_m^*C_n = |C_m^*C_n|\exp(i\vartheta_{mn})$ and Ω_{mn} stands for the Rabi frequency defined as

$$\Omega_{mn} = (\mathcal{E}_m - \mathcal{E}_n)/\hbar. \tag{26}$$

Also, in Eq. (24), $\bar{\Gamma}_{mn}$ is the mean of the widths of the corresponding interacting resonances,

$$\bar{\Gamma}_{mn} \equiv (\Gamma_m + \Gamma_n)/2. \tag{27}$$

B. Scattering problem

For the scattering problem, we suppose that the initial state of the particle $\Psi_s(x,0)$ satisfies the so-called quantum shutter setup [25], i.e.,

$$\Psi_s(x,0) = \begin{cases}\psi_0(x), & x<0\\ 0, & x>0\end{cases}. \tag{28}$$

Notice that, in contrast to the purely decaying case of the previous subsection where the initial state was seated inside the system, here the initial state is seated outside the interaction region. Under this condition, the formal time-dependent solution $\Psi(x,t)$ may be written as

$$\Psi_s(x,t) = \int_{-\infty}^{\infty} dk\;\phi_0(k)\psi^+(x;k)e^{-i\hbar k^2 t/2m}, \tag{29}$$

where $\phi_0(k)$ is the Fourier transform of the initial state Eq. (28) and $\psi^+(x;k)$ the corresponding scattering state of the problem

corresponding to incidence from left to right and normalized according to

$$\int_{-\infty}^{\infty} dx\ \psi^{+*}(x;k')\psi^{+}(x;k) = \delta(k-k').$$

As is well known, the scattering state $\psi^{+}(x;k)$ outside the potential region read

$$\psi^{+}(x,k) = \frac{1}{\sqrt{2\pi}} \begin{cases} e^{ikx} + \boldsymbol{r}(k)e^{-ikx}, & x \leqslant 0 \\ \boldsymbol{t}(k)e^{ikx}, & x \geqslant L \end{cases}, \quad (30)$$

where $\boldsymbol{r}(k)$ and $\boldsymbol{t}(k)$ stand, respectively, for the reflection and transmission amplitudes. The internal solution is related with the corresponding outgoing Green function of the problem as [17,26]

$$\psi^{+}_{\rm int}(x;k) = \left(\frac{\hbar^2}{2m}\right)\frac{2ik}{\sqrt{2\pi}}G^{+}(x,0;k), \quad 0 < x < L. \quad (31)$$

Following recent work by Cordero and García-Calderón [27], we may expand $G^{+}(x,0;k)\exp(-ikx)$ [instead of $G^{+}(x,0;k)$] over the resonance states to find

$$\psi^{+}_{\rm int}(x;k) = \frac{ik}{\sqrt{2\pi}}\sum_{n=-\infty}^{\infty}\frac{r_n(x)e^{-i\kappa_n x}}{k-\kappa_n}e^{ikx}, \quad 0 < x \leqslant L, \quad (32)$$

where

$$r_n(x) = \frac{u_n(0)u_n(x)}{\kappa_n}, \quad (33)$$

with κ_n and $u_n(x)$ being the nth complex pole and resonant state, respectively.

Substituting Eq. (32) into Eq. (29), and using the relationship

$$\frac{k}{k-\kappa_n} \equiv 1 + \frac{\kappa_n}{k-\kappa_n}, \quad (34)$$

one may write the time-dependent solution $\Psi_{\rm int}$ along the internal interaction region $0 \leqslant x \leqslant L$ as

$$\Psi_{\rm int}(x,t) = i\sum_{n=-\infty}^{\infty} r_n(x)e^{-i\kappa_n x}\Psi_f(x,t) + i\sum_{n=-\infty}^{\infty} r_n(x)\kappa_n Q_0(x,t;\kappa_n)e^{-i\kappa_n x}, \quad (35)$$

where

$$\Psi_f(x,t) = \frac{1}{\sqrt{2\pi}}\int_{-\infty}^{\infty} dk\ \phi_0(k)e^{ikx-i\hbar k^2 t/2m} \quad (36)$$

is the corresponding free evolution, and

$$Q_0(x,t;\kappa_n) = \frac{1}{\sqrt{2\pi}}\int_{-\infty}^{\infty} dk\ \phi_0(k)\frac{e^{ikx-i\hbar k^2 t/2m}}{k-\kappa_n} \quad (37)$$

is a term that depends on each complex pole κ_n of the system.

Let us consider the particular case in which the initial state is an incident cutoff Gaussian wavepacket. For this initial condition, one may write

$$\psi_0(x) = A_0\left(\frac{1}{2\pi\sigma^2}\right)^{1/4} e^{-(x-x_0)^2/4\sigma^2}e^{ik_0 x}, \quad (38)$$

where

$$A_0 = \left(\frac{2}{\operatorname{erfc}(x_0/\sqrt{2}\sigma)}\right)^{1/2}. \quad (39)$$

In the above expressions, $x_0 < 0$ and σ stand, respectively, for the center and the effective width of the Gaussian and we make use of $E_0 = \hbar^2 k_0^2/2m$, the energy of the wavepacket. The Fourier transform of Eq. (38) is given by

$$\phi_0(k) = \frac{1}{(2\pi)^{1/4}}\left(\frac{\sigma}{\omega(iz_0)}\right)^{1/2}\omega(iz), \quad (40)$$

where

$$z = \frac{x_0}{2\sigma} - i(k-k_0)\sigma, \quad (41)$$

and

$$z_0 = \frac{x_0}{\sqrt{2}\sigma}, \quad (42)$$

with $\omega(z)$ the Faddeyeva function [22,23].

Let us place the initial wave packet along the region $x < 0$. As pointed out above, here we shall be concerned with the physically relevant situation where the tail of the initial Gaussian wave packet is very small near the interaction region. It is then convenient to consider the symmetry relationship for the Faddeyeva function given by Eq. (19) and follow an argument given by Villavicencio *et al.* for the free and δ potential cases [28], which may be applied also to the interaction potential case [29], that consists in approximating $\omega(iz)$ as

$$\omega(iz) \approx 2e^{-z^2}, \quad (43)$$

provided that

$$\left|\frac{x_0}{2\sigma}\right| \gg 1. \quad (44)$$

The condition given by Eq. (44) is the usual condition used for scattering of Gaussian wavepackets. It simply means that initially the tail of the Gaussian wavepacket is negligible along the interaction potential region.

Substituting Eq. (43) into Eqs. (36) and (37) yields expressions satisfying the condition given by (44) that we denote, respectively, by $\Psi_f^a(x,t)$ and $Q_0^a(x,t;\kappa_n)$, and are given by [29]

$$\Psi_f^a(x,t) = \frac{1}{(2\pi)^{1/4}}\frac{1}{\sigma^{1/2}}\frac{e^{i(k_0x-\hbar k_0^2 t/2m)}e^{imx'^2/2\hbar t'}}{\sqrt{1+it/\tau}} \quad (45)$$

and

$$Q_0^a(x,t;\kappa_n) = -i\sigma\pi^{1/2}\sqrt{1+it/\tau}\,\Psi_f^a(x,t)\omega(iy_n'), \quad (46)$$

where the following quantities have been defined

$$\tau = \frac{2m\sigma^2}{\hbar}, \quad t' = t - i\tau, \quad x' = x - x_0 - \frac{\hbar k_0}{m}t, \quad (47)$$

and

$$y_n' = e^{-i\pi/4}\sqrt{\frac{m}{2\hbar t'}}\left[x' - \frac{\hbar\kappa_n'}{m}t'\right], \quad \kappa_n' = \kappa_n - k_0. \quad (48)$$

Let us now substitute Eq. (46) into Eq. (35) to find

$$\Psi^a_{\rm int}(x,t) = \Psi^a_f(x,t) \sum_{n=-\infty}^{\infty} ir_n(x)e^{-i\kappa_n x} [1 - i\sigma\pi^{1/2}\sqrt{1+it/\tau}\kappa_n\omega(iy'_n)]. \quad (49)$$

It follows then, using the symmetry property of the Faddeyeva function Eq. (19), that Eq. (49) may be written as

$$\Psi^a_{\rm int}(x,t) = \sum_{n=1}^{\infty} D_n u_n(x)e^{-i\mathcal{E}_n t/\hbar}e^{-\Gamma_n t/2\hbar} + I_n(x,t), \quad (50)$$

where D_n reads

$$D_n = 2\left(\frac{\pi}{2}\right)^{1/4}\sigma^{1/2}e^{-[i\kappa'_n x_0 + \kappa'^2_n\sigma^2]}u_n(0), \quad (51)$$

and $I_n(x,t)$ stands for the corresponding nonexponential contributions.

It may be shown that the internal time-dependent solution given by Eq. (49) behaves at asymptotic long times as $\Psi^a_{\rm int}(x,t) \sim t^{-3/2}$, in a similar fashion as occurs for the purely decaying case of the previous subsection.

It is worth pointing out that both the decaying solution given by Eq. (20) and the internal scattering solution given by Eq. (50) exhibit similar exponentially decaying terms, both being proportional to the resonant states $u_n(x)$, and expansion coefficients that depend on the corresponding initial states. Clearly, along the exponentially decaying regime one may write Eq. (50) as

$$\Psi^a_{\rm int}(x,t) \approx \sum_{n=1}^{\infty} D_n u_n(x)e^{-i\mathcal{E}_n t/\hbar}e^{-\Gamma_n t/2\hbar} \quad (52)$$

and derive analogous expressions to those given by Eqs. (22)–(27) (replacing the C' by the D') to describe Rabi oscillations in the decaying probability density of the quasistationary state formed by wavepacket scattering.

III. EXAMPLES AND DISCUSSION

In this section, we analyze the dynamical behavior of the decaying probability density in quantum wells of resonant tunneling structures for initial quantum states created both *inside* and *outside* the system. In the former case, which we refer to as the *purely decaying* case, the initial state $\Psi_0 \equiv \Psi(x,0)$ is a sine pulse of the form

$$\Psi(x,0) = \left(\frac{2}{w_0}\right)^{1/2} \sin[k_j(x - x_s) + j\pi/2], \quad (53)$$

for $|x - x_s| < w_0/2$ and zero elsewhere, where x_s refers to the center of a well of width w_0 and $k_j = j\pi/w_0$ with $j = 1,2,3,\ldots$. In the latter case, which we refer to as the *scattering and decay* case, we choose as initial incident state the cutoff Gaussian wavepacket given by Eq. (28) with $\Psi_0(x)$ given by Eq. (38). Under the condition of Eq. (44), it is easy to see that the quantity $A_0 \to 1$, and hence one may write

$$\Psi(x,0) = \begin{cases} (1/2\pi\sigma^2)^{1/4}e^{-(x-x_0)^2/4\sigma^2}e^{ik_0 x}, & x < 0 \\ 0, & x > 0 \end{cases}. \quad (54)$$

The above initial conditions have in common the fact that both involve a decay process; however, they correspond to different physical situations. For the initial condition Eq. (53), the decaying state is suddenly created inside the system as a pulse in one of the quantum wells of the system. In contrast, for the initial condition Eq. (54), the quantum wells of the system are initially empty, since the initial state originates outside the system and, hence, a time is required to build up the probability density to a maximum before the decay process begins [14,15].

In order to illustrate the comparison of the decay between an initially decaying state and a quasistationary state formed by scattering of wavepackets, we shall use two different resonant tunneling systems characterized by typical parameters of semiconductor heterostructures [8,30]. One of them is the simple case of a symmetrical double barrier resonant structure (DBRS) and the other is a quadruple-barrier resonant structure (QBRS). In the former we have the simplest situation of a decaying state trapped inside the lateral walls of the system where the probability density has a relatively simple form [31], while in the latter the situation is more complex with the probability density exhibiting an internal dynamics governed by the interference between resonant states [24,32].

A. Double barrier

We consider a symmetrical DBRS with parameters: barrier heights $V_0 = 230$ meV, barrier widths $b_0 = 5.0$ nm, well widths $w_0 = 5.0$ nm, electron effective mass $m^* = 0.067\,m_e$, with m_e being the free electron mass. As mentioned above, for the *purely decaying* problem, we choose the initial state [Eq. (53)], and for the *scattering and decay* problem, we consider an incident cutoff Gaussian wavepackets [Eq. (54)].

Figure 1 exhibits contour plots of $\ln|\Psi_d(x,t)|^2$ and $\ln|\Psi_s(x,t)|^2$ along the interaction region in units of the length L of the system as a function of time in terms of the lifetime unit $\tau_1 = \hbar/\Gamma_1$ (which corresponds to the longest time scale). Figure 1(a) exhibits the time evolution of decay for the *purely decaying* initial pulse [Eq. (53)] with parameters $j = 1$ and $x_s = 7.5$ nm, using the solution given by Eq. (14) and keeping the first few necessary terms of the sum. Figure 1(b) exhibits the formation and subsequent decay of a Gaussian wavepacket, which was seated initially at a distance $x_0 = -8\sigma$ from the DBRS with $\sigma = 5.0$ nm, using the formal solution for scattering, Eq. (49). The incidence energy is $E_0 = 80.11$ meV, which corresponds to the first resonance energy level $\mathcal{E}_1$ of the system. Despite the fact that the initial decaying states were produced quite differently in the *purely decaying* and the *scattering and decay* cases, a remarkable similarity in the dynamics exhibited in Figs. 1(a) and 1(b) is observed. The only difference that can be appreciated in Fig. 1(b) is the fast buildup process that occurs at short times and lasts a fraction of a lifetime τ_1. In the latter case, the initial decaying state was *asymmetrically* created by injecting the Gaussian wavepacket through the left barrier, and once the buildup is accomplished in a relatively short time scale τ_b, the decay evolves thereafter in a fashion very similar as for the *purely decaying* case shown in Fig. 1(a), escaping *symmetrically* via tunneling through the lateral barriers as if it were created inside. This shows the efficiency of the Gaussian packet scattering to create high-quality initial decaying states in DBRSs.

With the purpose to see what happens with an incident wavepacket spectrally broader in k space, we consider in

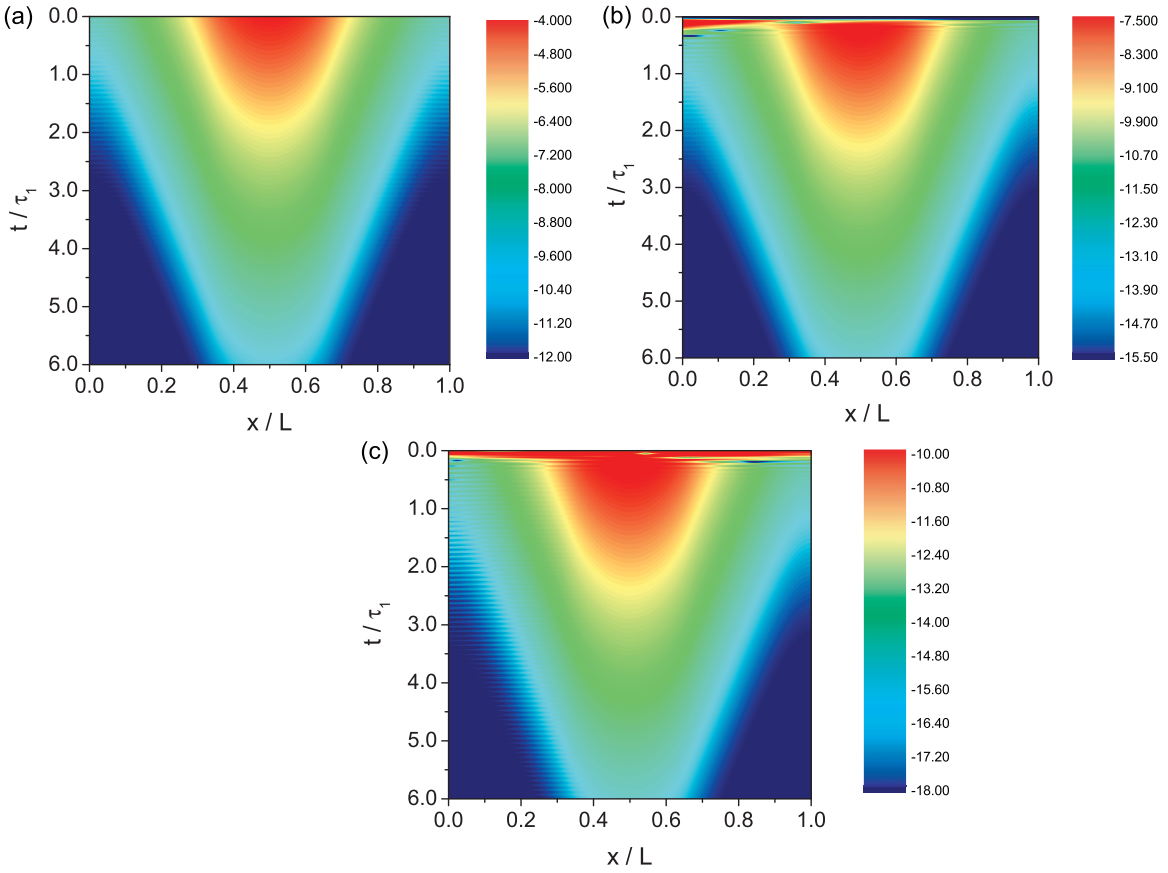

FIG. 1. (Color online) Contour plots of the natural logarithm of the probability density along the internal interaction region in units of the length L as time varies in units of the lifetime τ_1 for several initial states. Panel (a) shows the decay of a sine pulse seated initially in the well, whereas panels (b) and (c) exhibit, respectively, the formation and subsequent decay of Gaussian wave packets with $\sigma = 5.0$ nm and $\sigma = 0.5$ nm, seated initially at $x_0 = -8\sigma$ with the resonance energy of the system $E_0 = \mathcal{E}_1$. Notice here that in both cases the buildup time τ_b lasts just a fraction of a lifetime of the system. Notice also the similarity of the subsequent time evolution of decay between case (a) with cases (b) and (c).

Fig. 1(c) the resulting dynamics when using a spatially narrower incident Gaussian wavepacket of width $\sigma = 0.5$ nm, $x_0 = -8\sigma$, and the rest of the parameters as in Fig. 1(b). Also in this case, the dynamics of decay is quite similar to the purely decaying case of Fig. 1(a), with a short duration buildup process that now exhibits an oscillatory transient [more evident in the inset of Fig. 2(c). See below].

Let us now analyze the behavior of the time evolution of the decaying state in the full time domain, i.e., one that includes the whole exponential regime as well as the transition from exponential to nonexponential decay occurring at long times. In Figs. 2(a), 2(b), and 2(c) we show, respectively, plots of the corresponding natural logarithm of the probability densities as a function of time, at a fixed position x_f inside the system, for the three cases discussed previously in Fig. 1. Figure 2(a) yields a plot of $\ln |\Psi_d(x,t)|^2$ as a function of time t, in lifetime units, at the position $x_f = 7.5$ nm, which corresponds to both the middle of the system and the well. As we can see, the dynamical evolution of $\ln |\Psi_d(x_f,t)|^2$ exhibits an exponential decaying regime followed by a transition to a nonexponential regime governed by the inverse law t^{-3} [24,32]. It turns out that the real part of the overlap of the initial state $\Psi_d(x,0)$ with the lowest resonant state $u_1(x)$ is larger than the overlap corresponding with the rest of resonant states, namely, $\mathrm{Re}\, C_1^2 = 0.77$. This means, in view of Eq. (16), that the rest of resonant states share the remaining strength. Hence, one may conclude that in the *purely decaying* case, along the internal interaction region, the decaying quasistationary state is at a good approximation, proportional to the resonant state $u_1(x)$.

In order to compare the above purely decaying process with scattering and decay case, let us consider the situation in which the initial state is created outside the system using the cutoff wavepacket Eq. (54), with $\sigma = 5.0$ nm, $x_0 = -8\sigma$, and incidence energy $E = \mathcal{E}_1 = 80.11$ meV. We show in Fig. 2(b) the time evolution of $\ln |\Psi_s(x,t)|^2$ at the same fixed position $x_f = 7.5$ nm. As we can see, the dynamical behavior of $\ln |\Psi_s(x_f,t)|^2$ for the scattering case is qualitatively similar to the purely decaying case along the whole time domain. However, the differences can be appreciated in the upper inset of Fig. 2(b), where an amplification of the main graph was taken over a shorter time interval. Here, it is evident that a buildup process occurs at a relatively short time scale, which is the time required for the incident wavepacket to penetrate the system and fill up the well of the DBRS. Once the internal probability density reaches an absolute maximum (as a function of time), the decay process begins, following an exponential behavior until it

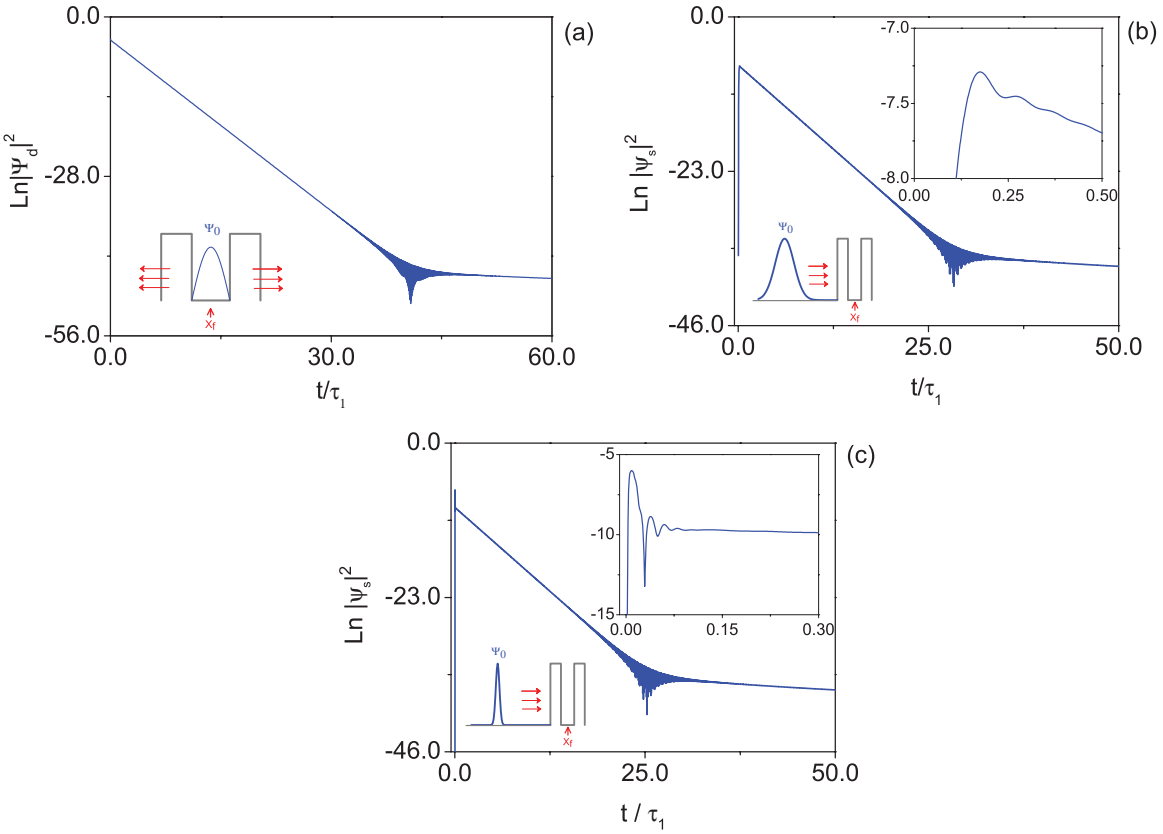

FIG. 2. (Color online) Plot of the natural logarithm of the probability density as a function of the time t at the center of the well ($x_f = 75$ nm) of the DBRS, for distinct initial states consisting of (a) a sine pulse that fits in the first well, (b) a cutoff Gaussian wavepacket of width $\sigma = 5.0$ nm, initial position $x_0 = -8.0\sigma$, incidence energy $E_0 = \mathcal{E}_1 = 80.11$ meV, and (c) a thinner cutoff Gaussian wavepacket of width $\sigma = 0.5$ nm and initial position $x_0 = -8.0\sigma$ and the same incidence energy. In cases (b) and (c), the upper inset is a zoom that illustrates the buildup that occurs before the decay process.

reaches a transition to the well known nonexponential regime. Figure 2(c) displays the values of $\ln|\Psi_s(x,t)|^2$ vs t/τ_1 for a thinner cutoff wavepacket (and hence with more spread in k space). The wavepackets parameters are $\sigma = 0.5$ nm and $x_0 = -8\sigma$. As we can appreciate in the upper inset, a transient occurs before establishment of the exponential part of the decay process. However, the decay process exhibits essentially the same form as in Fig. 2(b) along the whole time interval, showing that even in this case the scattering process is capable to effectively produce the quasistationary decaying state.

It is worth noticing that the deviation from exponential decay in Figs. 2(a), 2(b), and 2(c) occurs at different times, which indicates a dependence of the values of these transition times on the parameters of the corresponding initial states.

B. Quadruple barrier

As a second example we consider a quadruple-barrier resonant structure (QBRS) with barrier heights $V_0 = 200$ meV, barrier widths $b_0 = 4.0$ nm, and well widths $w_0 = 5.0$ nm. As in the previous example for the DBRS, we keep the same effective electron mass. For the *purely decaying* problem we choose the initial state [Eq. (53)], and for the *scattering and decay* problem we consider the initial Gaussian state [Eq. (54)] with $\sigma = 5.0$ nm.

Figure 3 exhibits contour plots of the natural logarithm of the probability density along the interaction region in units of the length L as a function of time in terms of the lifetime unit $\tau_1 = \hbar/\Gamma_1$. Figure 3(a) exhibits the time evolution of decay for the *purely decaying* initial pulse [Eq. (53)] with parameters $j = 1$ and $x_s = 6.5$ nm, the center of the first well from the left. On the other hand, Fig. 3(b) exhibits the formation and subsequent decay of the Gaussian wavepacket, which is seated initially at a distance $x_0 = -8\sigma$ from the QBRS. The corresponding incident energy is $E_0 = 66.46$ meV, which corresponds to the first resonance energy level $\mathcal{E}_1$ of the system. Notice that Fig. 3(b) exhibits a buildup time that lasts a fraction of a lifetime, as occurs also in the DBRS example. Subsequently, the decay process evolves in a fashion very similar to the *purely decaying* situation, as may be seen by comparison of Figs. 3(b) and 3(a). In both cases, the dynamics occur in the form of a *bouncing mode*, where the maximum of the probability density follows a back-and-forth motion inside the system that resembles the classical picture of a particle bouncing on the lateral walls. In fact, the dynamics is governed by a mixture of Rabi frequencies resulting from the interference between the relevant resonant states of the miniband. Therefore, the bouncing mode exhibited in the internal dynamics, despite its resemblance with the classical motion, is completely a quantum mechanical effect. Note also that this bouncing-like motion does not occur in a continuous fashion as in the case of a classical particle, instead it consists of a series of buildup processes repeated

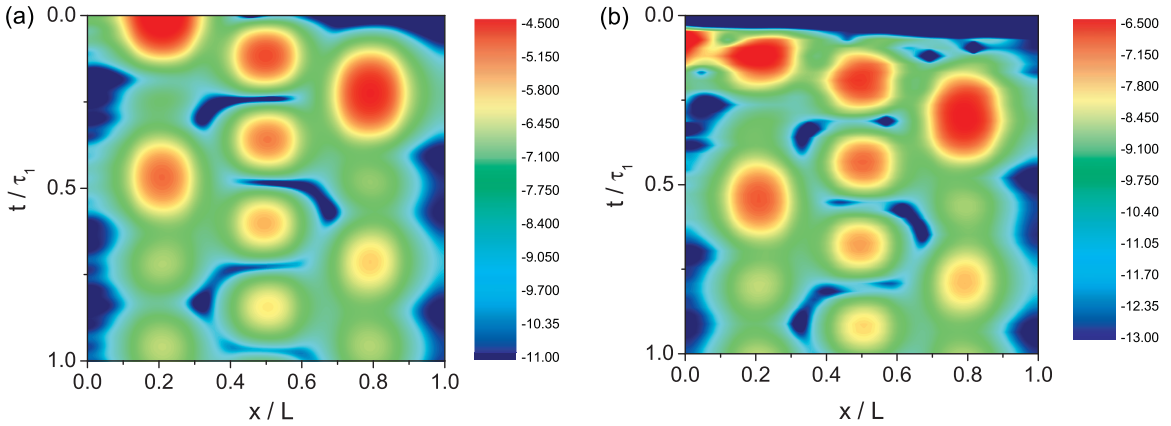

FIG. 3. (Color online) Contour plots of the natural logarithm of the probability density along the internal interaction region in units of the length L as time varies in units of the lifetime τ_1 of the QBRS. Panel (a) shows the decay of a sine pulse seated initially in the first well on the left, whereas panel (b) exhibits the formation and subsequent decay of a Gaussian wave packet with $\sigma = 5.0$ nm seated initially at $x_0 = -8\sigma$ with the resonance energy of the system $E = \mathcal{E}_1$. Notice that the buildup time lasts a fraction of a lifetime and that the time evolution of decay in both cases is quite similar. See text.

sequentially in the different wells. The probability density fades out in the classical forbidden regions (barriers) and reappears successively in the wells along the system from one side to the other. These peculiarities are characteristic features of these sorts of systems. They are quantum mechanically robust in the sense that they imprint on the decaying state a unique bouncing dynamics, and the process by which the initial state is formed is not essential to determine the ulterior behavior with time of the decaying state.

Figure 4 shows the comparison of the decaying probability density at the center of the first well of the same QBRS considered above for two different physical situations. In the first case, the initial state was created inside the system as a quantum box ground state centered in the first well as pictured in the lower inset of Fig. 4(a). In the second case, the initial state consists of an incident cutoff Gaussian wavepacket that comes from the left, as illustrated in the lower inset of Fig. 4(b). In both situations, the natural logarithm of the corresponding probability densities as a function of the time t/τ_1 (in lifetime units) is displayed at the fixed position $x_f = 6.5$ nm (center of the first well). The upper inset of each figure displays the values of the corresponding natural logarithm of the probability density in wider time intervals, so that the transition from exponential to nonexponential decay is clearly appreciated. The main graphs are the amplifications of the marked area in the upper left corner of these insets, and they show the detailed structure of the decaying probability density at the beginning of the exponential regime.

Simple visual comparison of Figs. 4(a) and 4(b) shows the strong similarity in the time evolution of the corresponding plots of the natural logarithm of the probability density, except for the small shift in Fig. 4(b) associated to the buildup time τ_b. Once the maximum value of the buildup of the quasistationary state in Fig. 4(b) is accomplished, the subsequent oscillatory pattern is quite similar to the one displayed in Fig. 4(a) corresponding to the purely decaying case. The buildup time τ_b can be obtained by measuring the shift between both curves. However, as discussed by Støvneng and Hauge in the DBRS [13], this quantity depends on external factors such as the initial position and width of the incident packet. In contrast,

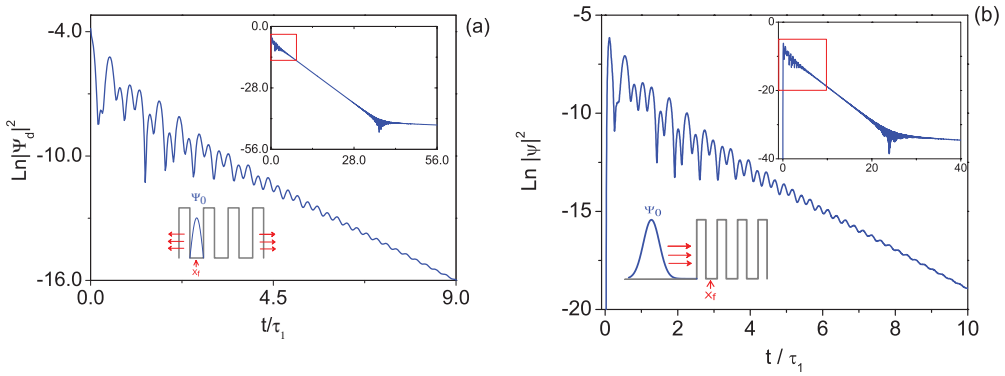

FIG. 4. (Color online) Plot of the natural logarithm of the probability density as a function of the time t in lifetime units at the center of the first well ($x_f = 6.5$ nm) of a QBRS, for an initial state consisting on: (a) a sine pulse in the first well and (b) a Gaussian wavepacket with initial position $x_0 < 0$ and incident energy $E = \mathcal{E}_1 = 66.46$ meV. The upper insets displays a similar calculation for a longer time interval. Note the transition from exponential to nonexponential decay occurs after many lifetimes.

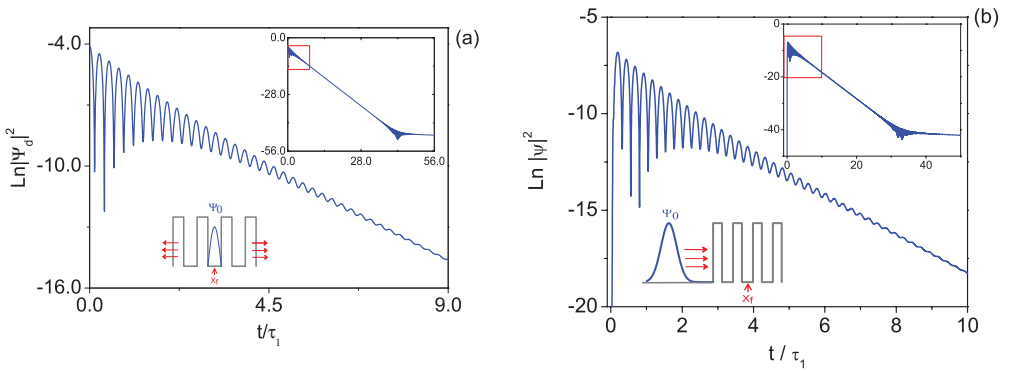

FIG. 5. (Color online) Plot of the natural logarithm of the probability density as a function of the time t in lifetime units at the center of the second well ($x_f = 15.5$ nm) of a QBRS, for an initial state consisting on: (a) a sine pulse in the second well, and (b) a Gaussian wavepacket with initial position $x_0 < 0$ and incident energy $E = \mathcal{E}_1 = 66.46$ meV. The insets display a similar calculation for a longer time interval.

the decay process in these few period resonant structures, is mainly governed by internal factors: the resonant states and their interferences.

Let us consider now the time evolution of the probability density at the center of the central well, namely, $x_f = 15.5$ nm. Figure 5 (a) illustrates the plot of $\ln|\Psi_d(x,t)|^2$ vs t/τ_1 for the case in which the initial state $\Psi_d(x,0)$ is a sine pulse centered in the second well, $x_s = 15.5$ nm, as pictured in the lower inset of that figure. For the scattering case, we show in Fig. 5(b) the corresponding plot of $\ln|\Psi_s(x,t)|^2$ vs t/τ_1 also in the center of the central well, for the initial state consisting on the incident cutoff Gaussian wavepacket (see picture in the lower inset) with the same system parameters and incidence energy as in Fig. 4(b). By simple inspection of the graphs, we can appreciate that, in both the *scattering and decay* and the *purely decaying* cases, the dynamical behavior of the corresponding probability densities is essentially the same, except again for a small shift in the graph of Fig. 5(b) due to the buildup occurring in the well before the decay process begins. The observed dynamics consist on a regular oscillatory pattern that is associated to spatial oscillations of the probability density between the central and lateral wells, which is related to a Rabi-type frequency involving the first and third resonant states of the system [24]. Interestingly, after a transient in which the decaying state is "prepared" through a scattering process, the dynamics exhibited in Fig. 5(b) follows exactly the same behavior of the *purely decaying* case depicted in Fig. 5(a). This occurs despite the fact that the buildup in the central well must wait for the arrival of the filtered components of the incident wavepacket across the two barriers on the left, and the buildup of the first well has been accomplished.

Figure 6(a) shows the comparison of the values of the natural logarithm of the probability density as a function of the time t at $x_f = x_1 = 6.5$ nm (center of the first well) and $x_f = x_2 = 24.5$ nm (center of the third well) when the initial state $\Psi_d(x,0)$ is placed in the first well, $x_s = 6.5$ nm. Both curves exhibit a similar oscillatory behavior, but one of them is shifted with respect to the other due to the buildup time of the probability density at the third well (initially empty), which is approximately half a period of the zigzag oscillatory pattern shown in the contour map of Fig. 3.

On the other hand, Fig. 6(b) shows the comparison of the same quantity as above at the same two fixed positions, $x_1 = 6.5$ nm and $x_2 = 24.5$ nm, for the scattering case in which initial state $\Psi_s(x,0)$ is the Gaussian wavepacket with incidence energy $E = \mathcal{E}_1 = 66.46$ meV. Here we observe a buildup process both in the first and the third well, since they were initially empty. Notice that the decay through the right edge of the system ($x = L$) must wait for the buildup of the third well as can be appreciated in the contour maps of Fig. 3;

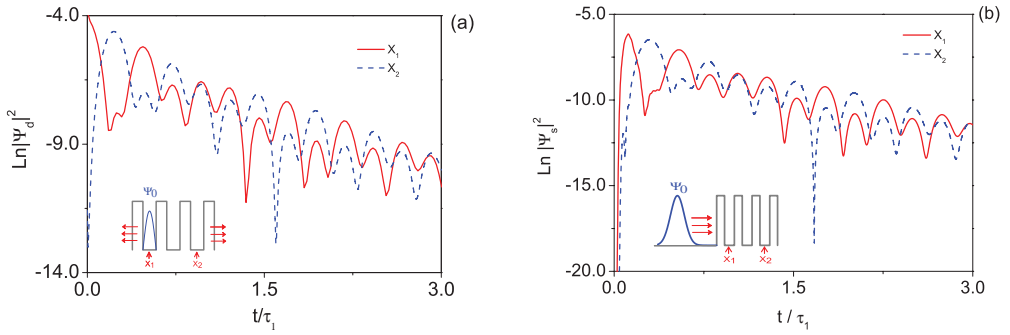

FIG. 6. (Color online) (a) Comparison of the natural logarithm of the probability density as a function of the time t in lifetime units at the center of the first well, $x_1 = 6.5$ nm (solid red line), and at the center of the third well, $x_1 = 24.5$ nm (dashed blue line) of a QBRS, for an initial state consisting on: (a) a sine pulse in the first well, (b) the same as above for a Gaussian wavepacket with initial position $x_0 < 0$ and incident energy $E = \mathcal{E}_1 = 66.46$ meV. The fixed positions of x_1 and x_2 are also indicated by arrows in the lower insets.

as we can see in these maps, the maximum leakage of the probability density through the last barrier occurs when the third well is full.

Notice that the transition times into the nonexponential behavior exhibited by the insets to Figs. 4 and 5 occurs, as in the case for double-barrier resonant tunneling systems, at different times, which indicates that these transition times depend on the parameters of the corresponding initial states.

IV. CONCLUDING REMARKS

We have presented a unified analytical description of decay and scattering processes by using the formalism of resonance states. The analytical expressions that describe the decay of both an arbitrary state seated initially within the system, the *purely decaying* case, and the formation and the decay of a quasistationary state within the system formed by scattering of a Gaussian wavepacket, the *scattering and decay* case, are given, respectively, by Eqs. (14) and (49) and alternatively, by Eqs. (20) and (50), which exhibit explicitly the corresponding exponentially decaying contributions.

A common feature of our calculations is that the formation of the quasistationary state is characterized by a fast buildup time of the order of a fraction of the lifetime of the corresponding system. The subsequent time evolution of the probability density is governed by the exponentially decaying term with the longest lifetime, usually that with $n = 1$, which may be preceded by interfering oscillating contributions (Rabi terms) for systems involving two or more wells. This regime is almost indistinguishable from the *purely decaying* case, as illustrated in Sec. III. Finally, we find that the deviation from the exponential behavior at long times has a dependence on the parameters of the corresponding initial states.

It is of interest to comment, that our calculations in the *scattering and decay* case refer to values of the width σ of the Gaussian wavepacket that are smaller or much smaller than the lengths of the systems considered. In k space, that means that the wavepacket interacts strongly, respectively, with a few or several resonance levels of the systems considered, as illustrated by the transient behavior in the insets to Figs. 2(b) and 2(c). In the limiting case of a very sharp wavepacket in k space, which implies an infinitely broad wavepacket in configuration space, a convenient form to study the buildup time is to consider a quantum shutter setup for a cutoff initial plane wave. A study of this problem for a double-barrier system has given a buildup time that corresponds to several lifetimes of the system [21]. Thus, in general, one may expect that the buildup time has a dependence on the width of the Gaussian wavepacket.

It is also of interest to point out that the buildup time of the probability density for the quasistationary state has a dependence on positions within the system, as illustrated in Figs. 6(a) and 6(b). This may have implication in studies on the transit time in resonant tunneling systems and certainly requires further studies that will be considered elsewhere.

Summing up, it is worth emphasizing that a characteristic quality of resonant tunneling structures is their robustness in the sense that the internal dynamics of decay is strongly governed by the resonance states of the system. That is, the resonance states are able to dictate essentially the same dynamics for initial pulses seated inside the system as well as for quasistationary states formed by scattering processes. This is evident by inspection of Eqs. (20) and (50) and by looking at the contour plots displayed by Figs. 1 and 3. For practical purposes, we may conclude that in the exponentially decaying regime, the *purely decaying* and *scattering and decay* cases are essentially indistinguishable.

ACKNOWLEDGMENTS

The authors acknowledge support as follows: S.C. a post-doctoral fellowship from DGAPA-UNAM; G.G-C., the partial financial support of DGAPA-UNAM under Grant No. IN112410; and R.R. and J.V., the partial financial support of Facultad de Ciencias UABC under Grant No. P/PIFI 2010-02MSU0020A-08.

[1] G. Gamow, Z. Phys. **51**, 204 (1928).
[2] R. W. Gurney and E. U. Condon, Phys. Rev. **33**, 127 (1929).
[3] G. Gamow, *Atomic Nuclei and Nuclear Transformations* (Clarendon Press, Oxford, 1937).
[4] J. M. Blatt and V. F. Weisskopf, *Theoretical Nuclear Physics* (John Wiley & Sons, New York, 1952).
[5] L. A. Khalfin, Sov. Phys. JETP **6**, 1053 (1958).
[6] S. R. Wilkinson, C. F. Bharucha, M. C. Fischer, K. W. Madison, P. R. Morrow, Q. Niu, B. Sundaram, and M. G. Raizen, Nature (London) **387**, 575 (1997).
[7] C. Rothe, S. I. Hintschich, and A. P. Monkman, Phys. Rev. Lett. **96**, 163601 (2006).
[8] D. K. Ferry and S. M. Goodnik, *Transport in Nanostructures* (Cambridge University Press, Cambridge, 1997).
[9] A. Chomette, B. Deveaud, A. Regreny, and G. Bastard, Phys. Rev. Lett. **57**, 1464 (1986).
[10] M. Tsuchiya, T. Matsusue, and H. Sakaki, Phys. Rev. Lett. **59**, 2356 (1987).
[11] K. Leo, J. Shah, E. O. Göbel, T. C. Damen, S. Schmitt-Rink, W. Schäfer, and K. Köhler, Phys. Rev. Lett. **66**, 201 (1991).
[12] H. Guo, K. Diff, G. Neofotistos, and J. D. Gunton, Appl. Phys. Lett. **53**, 131 (1988).
[13] J. A. Støvneng and E. H. Hauge, Phys. Rev. B **44**, 13582 (1991).
[14] Y. G. Peisakhovich and A. A. Shtygashev, Phys. Rev. B **77**, 075326 (2008).
[15] Y. G. Peisakhovich and A. A. Shtygashev, Phys. Rev. B **77**, 075327 (2008).
[16] G. García-Calderón, Adv. Quant. Phys. **60**, 407 (2010).
[17] G. García-Calderón, AIP Conf. Proc. **1334**, 84 (2011).
[18] R. G. Newton, *Scattering theory of Waves and Particles* (Spirnger-Verlag, Berlin, 1982).
[19] G. García-Calderón, Nucl. Phys. A **261**, 130 (1976).
[20] G. García-Calderón, *Resonant States and the Decay Process: Symmetries in Physics* (Springer-Verlag Berlin, 1992), Chap. 17, p. 252.

[21] G. García-Calderón and A. Rubio, Phys. Rev. A **55**, 3361 (1997).
[22] V. N. Faddeyeva and M. N. Terentev, *Tables of Values of the Function* $\omega(z) = e^{-z^2}(1 + \frac{2i}{\sqrt{\pi}} \int_0^z e^{t^2} \mathrm{d}t)$ *for Complex Argument,* edited by V. A. Fock (Pergamon, London, 1961).
[23] M. Abramowitz and I. Stegun, *Handbook of Mathematical Functions* (Dover, New York, 1968).
[24] G. García-Calderón, R. Romo, and J. Villavicencio, Phys. Rev. A **79**, 052121 (2009).
[25] N. Yamada, G. García-Calderón, and J. Villavicencio, Phys. Rev. A **72**, 012106 (2005).
[26] G. García-Calderón, Solid State Commun. **62**, 441 (1987).
[27] S. Cordero and G. García-Calderón, J. Phys. A: Math. Theor. **43**, 415303 (2010).
[28] J. Villavicencio, R. Romo, and E. Cruz, Phys. Rev. A **75**, 012111 (2007).
[29] S. Cordero and G. García-Calderón, J. Phys. A: Math. Theor. **43**, 185301 (2010).
[30] T. C. L. G. Sollner, W. D. Goodhue, P. E. Tannenwald, C. D. Parker, and D. D. Peck, Appl. Phys. Lett. **43**, 588 (1983).
[31] G. García-Calderón and J. Villavicencio, Phys. Rev. A **73**, 062115 (2006).
[32] G. García-Calderón, R. Romo, and J. Villavicencio, Phys. Rev. B **76**, 035340 (2007).